TRANSPORT AND ELECTRONIC PROPERTIES OF THE GaAs ALD-FET

O. Oubram [1, *], L. M. Gaggero-Sager [2], O. Navarro [1], and M. Ouadou [3]

[1]Instituto de Investigaciones en Materiales, Universidad Nacional Autónoma de México, Apartado Postal 70-360, México D.F. 04510, Mexico

[2]Facultad de Ciencias, Universidad Autónoma del Estado de Morelos, Av. Universidad 1001, Col. Chamilpa, 62210 Cuernavaca, MOR., Mexico

[3]LRIT-GSCM, Faculté des Sciences, 4 Avenue Ibn Battouta B.P. 1014 RP, Rabat, Morocco

Abstract—According to the scaling-down theory, the ALD-FET (Atomic Layer Doping-Field Effect Transistor) structure has attracted a lot of attention in view of its uses for developing devices with very short channels and for achieving very-high-speed operation. Therefore, there is a strong need to obtain an accurate understanding of carrier transport (mobility and conductivity) in such devices. In this work, we report the carrier transport based on the electronic structure of devices. Our results include analytical expressions of both mobility and conductivity. Our analytical expressions for the mobility and conductivity allow us to analyze transport in ALD-FET. We report regions where this device operates in digital and analogue mode. These regions are delimited in terms of intrinsic and extrinsic parameters of the system. The width of the Ohmic region as well as the NDR (Negative Differential Resistance) properties of the system are also characterized.

1. INTRODUCTION

Research and development of new semiconductor devices which enable ultrahigh speed operation and/or ultrahigh density memory are

strongly required. Devices with these characteristics are essential for future highly intelligent information and telecommunication systems. In order to make such high performance devices, the technology for δ-FET structures should be developed parallel to the improvement of conventional technologies. The use of this type of doping in semiconductor devices yields a great improvement in the performance of ultra high frequency optoelectronic devices [1]. Among the advantages of δ-FET are a high concentration of the quasi-2DEG (two-Dimensional Electronic Gas), a high breakdown voltage of the Schottky contact, and a narrow distance of the 2DEG from the gate and high transconductance [2–5]. These FETs will also offer a very high operating frequency and a very flat transconductance region [6–10], which is ideal for low distortion power amplification and a high electron mobility transistor due to the proximity of the delta channel to the gate [9, 11, 12].

The system which we are interested in is the GaAs ALD-FET. It was originally proposed by Yamagachi et al. [13]. When compared to conventional FET, a higher transconductance and high intrinsic transconductance are expected in ALD-FET [11, 14]. Furthermore, the statistical fluctuation of impurity atoms in the highly doped ALD layer is negligible. In addition, the fluctuation of doped atoms in the substrate does not cause serious problems [15].

ALD-FET (Figure 1) is a field effect transistor in which the channel is formed by growing an n-type Si δ-doped well and a p-type δ-doped barrier. These two wells are placed between the terminals of the source and the drain of a regular GaAs field effect transistor [16]. The presence of this n-type quantum well produces a localized 2DEG,
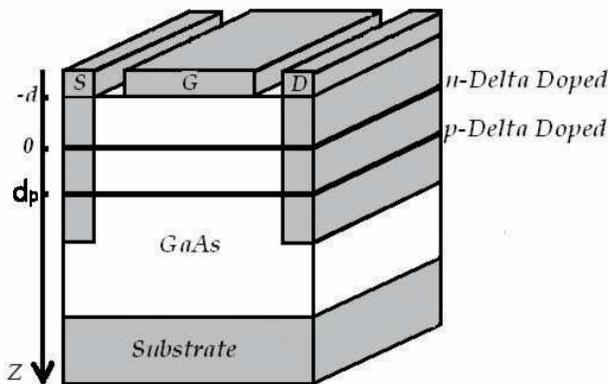
Figure 1. Cross-section of ALD-FET in GaAs.

which participates directly in the conduction channel [4, 17, 18]. On the other hand, the presence of the p-type quantum well produces a two-dimensional gas of holes (2DHG) and increase the electronic confinement in the n-type δ-doped quantum well. The inclusion of the barrier p-doped suppresses the punchthrough between source and drain as well as the transconductance keeps high [19].

Carrier mobility is an essential tool for understanding transport phenomenon. The transport properties of ALD-FET will be studied in two different ways. The first one requires calculations of the electronic structure, as was done in a previous study on δ-FET, ALD-FET and δ-MIGFET (δ-Multiple Independent Gate Field Effect Transistor) [20–24]. The second one uses the Thomas-Fermi approach, a method which does not require calculation of the electronic structure (eigenfunctions, eigenvalues). It found that the analytical expression for transport is a good tool to predict transport behavior in this device. Also, some electrical properties are characterized such as the width of the Ohmic region and the regime where the system has as a negative differential resistance. Finally, the regions where the system is operating in digital and analogue mode in terms of the ALD-FET parameters are delimited.

2. THEORETICAL BACKGROUND

The δ-doping technique allows to obtain an extremely sharp doping profile and a high-density-doped layer, which is of great interest [5, 25–29]. The potential of this system is formed by a metal-semiconductor contact (Schottky barrier), followed by the n-type δ-doped quantum-well system and another of the p-type. The presence or not of a confined electronic gas depends on the parameters used in the construction of the system.

If there is an electronic confinement, the model for describing the conduction band of the semiconductor in the ALD-FET system is described by the depletion region approach in the proximity of the metal-semiconductor contact [30],

$$V_{dep}(z) = \frac{2\pi e^2}{\epsilon_r} N_d (z + d - l)^2, \tag{1}$$

where N_d is the background impurity density; ϵ_r is the electric permittivity constant of GaAs; d is the distance at which the n-type δ-doped well is positioned; and l is the screening distance for the electric field.

In a region far from the interface, the δ-doped well potential is

described within a self-consistent Thomas-Fermi approach [31] by:

$$V_n(z) = -\frac{\alpha_n^2}{(\alpha_n|z| + z_{0n})^4}, \tag{2}$$

with $\alpha_n = 2/(15\pi)$ and $z_{0n} = (\alpha_n^3/\pi N_{2d})^{1/5}$, N_{2d} is the two-dimensional impurity density of the n-type δ-doped quantum-well.

The potential describes the p-type δ-doped quantum well centered at $z = d_p$. The confining potential can be written as [32]:

$$V_p(z) = \frac{\beta^2}{(\beta|z - d_p| + z_{0p})^4}, \tag{3}$$

here $\beta = 2m_a^{\frac{3}{2}}/15\pi$ with $m_a = [1 + (m_{lh}/m_{hh})^{\frac{3}{2}}]^{\frac{2}{3}}$, $m_{hh} = 0.51 \times m_0$ is the mass of the heavy hole and $m_{lh} = 0.082 \times m_0$ is the mass of the light hole for GaAs. $z_{0p} = (\beta^3/\pi p_{2d})^{1/5}$ with p_{2d} the bidimensional impurity density of the p-type δ-doped quantum-well.

So, the total potential is then

$$\begin{aligned} V(z) = {}& \frac{2\pi e^2}{\epsilon_r}N_d(z + d - l)^2\theta(l - z) \\ & + \left(-\frac{\alpha_n^2}{(\alpha_n|z| + z_{0n})^4} + \frac{\beta^2}{(\beta|z - d_p| + z_{0p})^4}\right)\theta(l_p - z), \end{aligned} \tag{4}$$

where l_p is the depletion region width and $V(l_p) = 0$.

We calculate the eigenvalues and eigenfunctions of the Schrödinger equation

$$-\frac{\hbar^2}{2m_e^*}\frac{d^2F_i(z)}{dz^2} + V(z)F_i(z) = E_iF_i(z), \tag{5}$$

where $F_i(z)$ is the ith eigenfunction of the n-type δ-doped and E_i is the ith eigenvalue.

3. TRANSPORT PROPERTIES

Based on the Thomas-Fermi approach to this ALD-FET, in the following, the electron transport properties of the system are studied. Only, the ionized donor scattering mechanism is considered because it is the most important at low temperature. The Coulomb scattering potential due to the ionized impurities is considered as distributed randomly in the doped layer. The relative mobility is defined as [33]:

$$\mu_{rel} = \frac{\mu^{V_c}}{\mu^{V_c=0}} = \frac{\int\int \rho_e^{V_c=0}(z')\rho_{imp}^{V_c=0}(z)|z - z'|dzdz'}{\int\int \rho_e^{V_c}(z')\rho_{imp}^{V_c}(z)|z - z'|dzdz'}, \tag{6}$$

$\rho_e^{V_c}(z')$ is the electronic density of n-delta doped with V_c the contact potential of the gate and $\rho_{imp}^{V_c}(z)$ is the impurity density of n-delta doped.

Using $\rho_{imp}^{V_c} = N_{2d} \times \delta(z)$, where $\delta(z)$ is the Dirac function, the relative mobility can be written as follows

$$\mu_{rel} = \frac{\int \rho_e^{V_c=0}(z)|z|dz}{\int \rho_e^{V_c}(z)|z|dz}. \tag{7}$$

Within the effective mass theory at $T = 0\,\mathrm{K}$:

$$\rho_e(z) = \frac{em^*}{\pi\hbar^2}\Sigma_1^{n_e}|F_i(z)|^2(E_f - E_i)\theta(E_f - E_i), \tag{8}$$

where E_f is the Fermi level, n_e is the electronic state number and θ is the unit-step function. So, the relative mobility is:

$$\mu_{rel} = \frac{\mu^{V_c}}{\mu^{V_c=0}} = \frac{\Sigma_1^{ne}\int |F_i^{V_c=0}(z')|^2 \left(E_f^{V_c=0} - E_i^{V_c=0}\right)|z'|dz'}{\Sigma_1^{ne}\int |F_i^{V_c}(z')|^2 \left(E_f^{V_c} - E_i^{V_c}\right)|z'|dz'}. \tag{9}$$

Here $F_i^{V_c}(z')$, $E_f^{V_c}$ and $E_i^{V_c}$ are the envelope function, the Fermi level and the ith energy level of n-delta doped, respectively.

The relative electronic density is defined as

$$n_{rel} = \frac{n^{V_c}}{n^{V_c=0}} = \frac{\Sigma_1^{ne}(E_f^{V_c} - E_i^{V_c})}{\Sigma_1^{ne}(E_f^{V_c=0} - E_i^{V_c=0})}. \tag{10}$$

Therefore, the relative conductivity $\sigma_{rel} = n_{rel} \times \mu_{rel}$ is:

$$\sigma_{rel} = \frac{\Sigma_1^{ne}(E_f^{Vc} - E_i^{Vc}) \times \Sigma_1^{ne}\int |F_i^{Vc=0}(z')|^2 \left(E_f^{Vc=0} - E_i^{Vc=0}\right)|z'|dz'}{\Sigma_1^{ne}(E_f^{Vc=0} - E_i^{Vc=0}) \times \Sigma_1^{ne}\int |F_i^{Vc}(z')|^2 \left(E_f^{Vc} - E_i^{Vc}\right)|z'|dz'}. \tag{11}$$

To calculate μ_{rel}, n_{rel} and σ_{rel} it is necessary to know the eigenvalues and eigenfuncions of the system.

In order to obtain an analytical expression for the conductivity, the Thomas-Fermi approach will be used, it means

$$\rho_e(z) = \frac{1}{2\pi e^2\hbar^2}(2m^*)^{\frac{3}{2}}(E_f - V(z))^{\frac{3}{2}}, \tag{12}$$

where, it is assumed that electrons are in the classical limit, then $z \in [l_p, L']$ and $V(z)$ is given by (4). In this limit, the analytical relative mobility for V_c is written as:

$$\mu'_{rel} = \frac{\mu'^{V_c}}{\mu'^{V_c=0}} = \frac{\int_{l_p}^{L'}\int \rho_e^{V_c=0}(z)\rho_{imp}^{V_c=0}(z')|z - z'|dzdz'}{\int_{l_p}^{L'}\int \rho_e^{V_c}(z)\rho_{imp}^{V_c}(z')|z - z'|dzdz'}, \tag{13}$$

with $l_p < 0$, $V(l_p) = V(L') = 0$ (see Figure 2) and $E_f = 0\,\mathrm{meV}$ in GaAs.

In a first approximation only the δ-doped potential effect will be considered when $z \in [l_p, L']$ then:

$$V(z) \simeq V_n(z) = -\frac{\alpha_n^2}{(\alpha_n |z| + z_{0n})^4}. \tag{14}$$

Using Equations (7), (12) and (14), μ'_{rel} is:

$$\mu'_{rel} = \frac{\left[\int_{l_p}^{L'} (E_f - V_n(z)) |z| dz\right]^{V_c = 0\,\mathrm{meV}}}{\left[\int_{l_p}^{L'} (E_f - V_n(z)) |z| dz\right]^{V_c}}. \tag{15}$$

The analytical expression for the relative mobility can be written as:

$$\mu'_{rel} = \left[\frac{1}{1 - \frac{a^4}{2}\left(\frac{5l_p - a}{(l_p - a)^5} + \frac{5L' + a}{(L' + a)^5}\right)}\right]^{V_c}, \tag{16}$$

with $a = \frac{z_{0n}}{\alpha_n}$.

Using the same approximation as before, the analytical expression for the relative electronic density is

$$n'_{rel} = \frac{\rho_e^{V_c}}{\rho_e^{V_c = 0}} = \left[1 + \frac{a^5}{(l_p - a)^5} - \frac{a^5}{(L' + a)^5}\right]^{V_c}. \tag{17}$$

Therefore, the relative analytical expression for the conductivity, $\sigma'_{rel} = n'_{rel} \times \mu'_{rel}$ will be:

$$\sigma'_{rel} = \left[\frac{(l_p - a)^5 (L' + a)^5 + a^5 \left[(L' + a)^5 - (l_p - a)^5\right]}{(l_p - a)^5 (L' + a)^5 - \frac{a^4}{2}\left[(5l_p - a)(L' + a)^5 + (5L' - a)(l_p - a)^5\right]}\right]^{V_c}. \tag{18}$$

4. RESULTS AND DISCUSSION

The starting parameters for ALD-FET in GaAs are: $m^* = 0.067 \times m_0$, $\epsilon_r = 12.5$, $N_{2d} = 7.5 \times 10^{12}\,\mathrm{cm}^{-2}$ and $N_d = 1 \times 10^{18}\,\mathrm{cm}^{-3}$.

Figure 2 shows the confining potential and the sub-band energies with their envelope wave functions. The results were obtained using Thomas-Fermi model with $N_{2d} = 7.5 \times 10^{12}\,\mathrm{cm}^{-2}$ and $p_{2d} = 5 \times 10^{13}\,\mathrm{cm}^{-2}$, the background impurity $N_d = 10^{18}\,\mathrm{cm}^{-3}$ at $T = 0\,\mathrm{K}$. n-type δ-doped quantum-well is located at $300\,\mathrm{\mathring{A}}$ from the interface and p-type delta doped barrier is located at $200\,\mathrm{\mathring{A}}$ from n-type delta
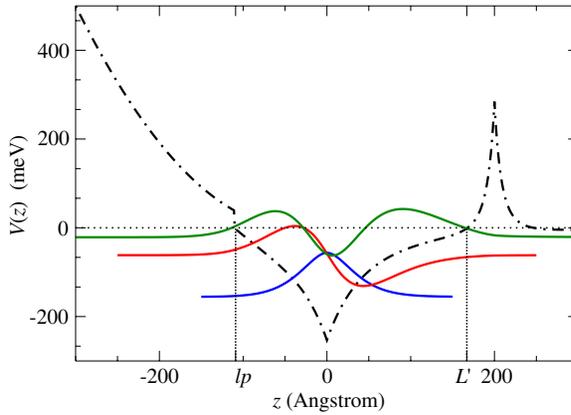
Figure 2. Conduction band, eigenvalues and eigenfunctiones, energies in meV for $V_c = 500 \, \text{meV}$, $N_{2d} = 7.5 \times 10^{12} \, \text{cm}^{-2}$, $p_{2d} = 5 \times 10^{13} \, \text{cm}^{-2}$, $d_p = 200 \, \text{Å}$ in GaAs in ALD-FET.

Table 1. Energy levels (E_0, E_1, E_2) for different values of p-delta doped concentration, $d_p = 200 \, \text{Å}$ and for $V_c = 500 \, \text{meV}$.

$p_{2d} \, (\text{cm}^{-2})$	$E_f - E_0 \, \text{meV}$	$E_f - E_1 \, \text{meV}$	$E_f - E_2 \, \text{meV}$
5×10^{12}	154.8	57.14	14.5
10×10^{12}	154.8	57.08	13.68
5×10^{13}	154.8	56.94	11.88

well. Dashed curve represents the obtained confining potential profile and solid curves represent the eigenfunctions with their eigenvalues. Moreover, Figure 2 shows eigenvalues, $E_0 = -154.8 \, \text{meV}$, $E_1 = -56.94 \, \text{meV}$ and $E_2 = -11.88 \, \text{meV}$ and the Fermi level is taken close to the bottom of conduction band for GaAs. The eigenfunctions and eigenvalues represent the starting point in the calculations of transport phenomena.

The influence of p-type δ-doped barrier on the energy levels can be seen in Table 1. The fundamental state does not feel the effects of the barrier, $E_f - E_0 = 154.8 \, \text{meV}$. In contrast, the superior levels feel it. Specially, the upper level decreases rapidly from $E_f - E_2 = 14.5 \, \text{meV}$ (for $5 \times 10^{12} \, \text{cm}^{-2}$) to $E_f - E_2 = 11.88 \, \text{meV}$ (for $5 \times 10^{13} \, \text{cm}^{-2}$). We adopt the transfer matrix method in order to calculate the eigenvalues [34–39].

The energy variation levels as a function of the contact voltage V_c is represented in Figure 3. The fundamental state is almost stable at
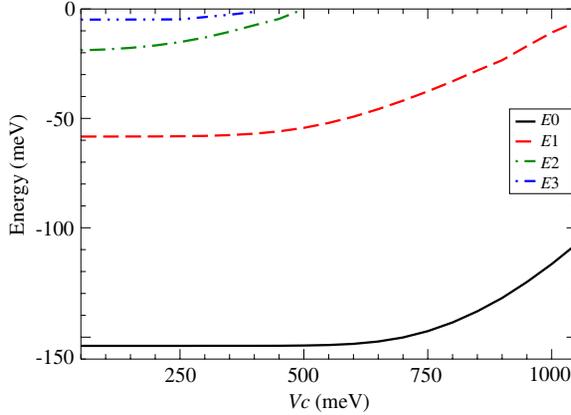
Figure 3. Electron level structure versus V_c in ALD-FET in GaAs for $d_p = 300$ Å, $N_{2d} = 7.5 \times 10^{12}\,\mathrm{cm}^{-2}$, $p_{2d} = 5 \times 10^{13}\,\mathrm{cm}^{-2}$.

a value around $-155.6\,\mathrm{meV}$ when $V_c < 550\,\mathrm{meV}$, the second level as well at a value around $-64.5\,\mathrm{meV}$ when $V_c < 400\,\mathrm{meV}$. Superior energy levels feel the effect when the contact potential increases. On the other hand, the contact potential severely affects the superior levels and the fundamental state when $V_c > 550\,\mathrm{meV}$ also. It is observed that the number of levels decreases when increasing V_c. For $V_c < 500\,\mathrm{meV}$ it has 4 energy levels, and for $V_c > 500\,\mathrm{meV}$ it has 3 levels. In other words, the electrons escaping is visible in the upper level. This observation will help us to explain later the transport phenomena.

Let us analyze the difference between μ_{rel} and σ_{rel}, calculated using the electronic structure, compared with the results coming from the analytical expression for these two transport properties.

Figure 4 shows the behavior of μ_{rel} and the analytical expression for this mobility μ'_{rel} as a function of gate potential when the inter-well is 300 Å. The dashed curve displays analytical calculations using expression (16). The solid curve is obtained using electronic structure and calculated with (9). The solid curve shows two regions: The first one is from $50\,\mathrm{meV}$ to $500\,\mathrm{meV}$, and the second one is from $500\,\mathrm{meV}$ to $1000\,\mathrm{meV}$. These regions show up when the states number is changing. The first region has 4 energy levels, and the second one has three. The dashed curve shows how the relative analytical mobility increases and its linear behavior.

Table 2 compares both transport calculations. Four representative potentials that characterize their evolution are analyzed. Table 2 shows a comparison of the mobility calculation between μ_{rel} and μ'_{rel} for different values of the contact potential.
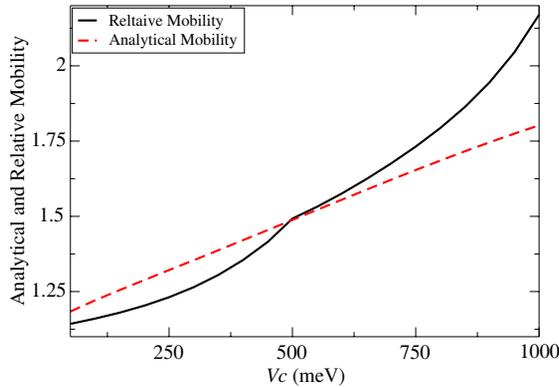
Figure 4. Relative and analytical mobility versus potential gate in ALD-FET in GaAs for $d_p = 300\,\text{Å}$, $N_{2d} = 7.5 \times 10^{12}\,\text{cm}^{-2}$, and $p_{2d} = 5 \times 10^{13}\,\text{cm}^{-2}$.

Table 2. Fluctuation percentage between both expressions of transport phenomenon for different values of gate potential V_c, $d_p = 300\,\text{Å}$, $N_{2d} = 7.5 \times 10^{12}\,\text{cm}^{-2}$ and for $p_{2d} = 5 \times 10^{13}\,\text{cm}^{-2}$.

V_c: Gate potential	250 meV	500 meV	750 meV	1000 meV
$\left\| \frac{\mu_{rel} - \mu'_{rel}}{\mu_{rel}} \right\| \times 100$	7	0.3	4.5	16.6
$\left\| \frac{\sigma_{rel} - \sigma'_{rel}}{\sigma_{rel}} \right\| \times 100$	3.5	3.4	3.3	1

It can be observed that the fluctuation does not exceed 7 percent at $V_c = 250\,\text{meV}$ and at $V_c = 500\,\text{meV}$, and it is less than 17 percent at $V_c = 750\,\text{meV}$ and at $V_c = 1000\,\text{meV}$. Fluctuation between both expressions μ_{rel} and μ'_{rel} is due to the approach considered in the computing of analytical mobility. The result can be improved, if more parameters of the system are considered. It can be concluded that the analytical mobility looks like a perfectly good tool to predict the tendency of mobility while the contact potential is below to 750 meV.

In Figure 5, the results of the conductivity obtained by two different forms are presented: a) -Solid curve shows the results obtained using expression (11). b) -Dashed curve shows the results obtained using the analytical expression (18).

In the solid curve, the conductivity can be subdivided in two intervals, for $V_c < 500\,\text{meV}$ and for 500 meV to 1000 meV. In each interval, the relative conductivity can be approximated by a parabolic curve with different curvature.
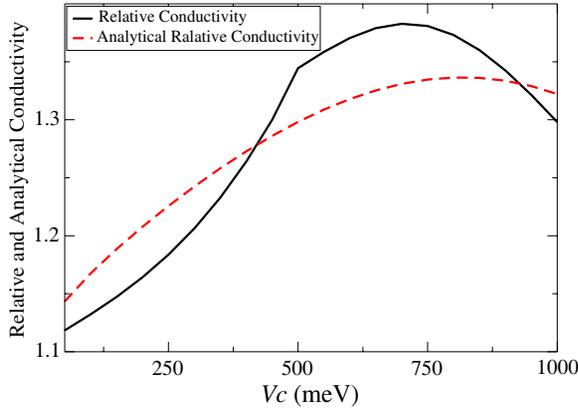
Figure 5. Relative and analytical conductivity versus potential gate in ALD-FET in GaAs for $d_p = 300\,\text{Å}$, $N_{2d} = 7.5 \times 10^{12}\,\text{cm}^{-2}$, and $p_{2d} = 5 \times 10^{13}\,\text{cm}^{-2}$.

Table 2 also shows the fluctuation between the relative conductivity $(\sigma_{rel}, \sigma'_{rel})$. At $V_c = 250\,\text{meV}$, $500\,\text{meV}$, $750\,\text{meV}$, $1000\,\text{meV}$, the fluctuation is less than 4 percent. The previous results allow us to consider that the analytical conductivity (σ'_{rel}) is in accordance with the first form (σ_{rel}), and it is a good approximation to estimate the relative conductivity.

Finally, the analytical conductivity is a good and fast tool to calculate and to get a good idea about the behavior of conductivity without calculating the eigenvalues and eigenfunctions.

Figures 6 and 7 show calculation of the transport phenomenon of ALD-FET using the result of the electronic structure. The calculation was made for two inter-wells distances at $100\,\text{Å}$ and $600\,\text{Å}$. The bi-dimensional densities are fixed at $N_{2d} = 7.5 \times 10^{12}\,\text{cm}^{-2}$ and at $p_{2d} = 5 \times 10^{13}\,\text{cm}^{-2}$. In Figure 6, the mobility shows two different interesting behaviors: The first one is between $100\,\text{meV}$ ($100\,\text{meV}$) and $1150\,\text{meV}$ ($1000\,\text{meV}$), where it has the mobility ratio rises mildly and so does from 1.07 (1.38) to 1.94 (3.1) (respectively). The second one is between $1150\,\text{meV}$ ($1000\,\text{meV}$) and $1300\,\text{meV}$ ($1300\,\text{meV}$), where the mobility increases rapidly and rises also from 1.9 (2.06) to 3.0 (4.52) (respectively).

It can be seen that contact potential affects more the mobility ratio when V_c is superior to $1150\,\text{meV}$ ($1000\,\text{meV}$). The mobility is multiplied by a factor of 2, when the p-type δ-doped is close to the conduction channel (n-type δ-doped). The different transitions in the mobility evolution are explained by changing the number of states in n-delta doped quantum well.
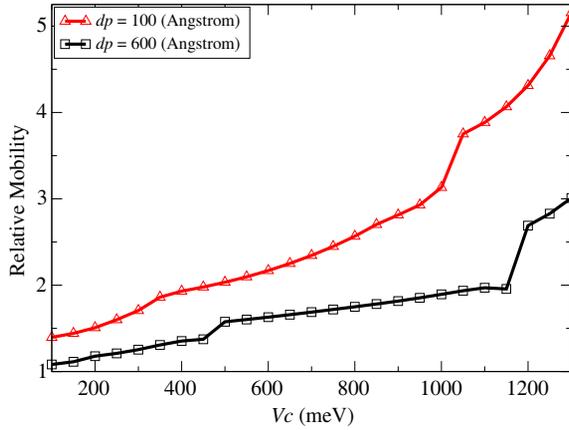
Figure 6. Relative mobility as a function of potential of contact for two values of inter-well distance between the n-type well and the p-type barriers in ALD-FET in GaAs for $N_{2d} = 7.5 \times 10^{12} \, \mathrm{cm}^{-2}$, $p_{2d} = 5 \times 10^{13} \, \mathrm{cm}^{-2}$, $d_p = 100 \, \mathring{\mathrm{A}}$ (triangle up symbol), $d_p = 600 \, \mathring{\mathrm{A}}$ (square symbol).
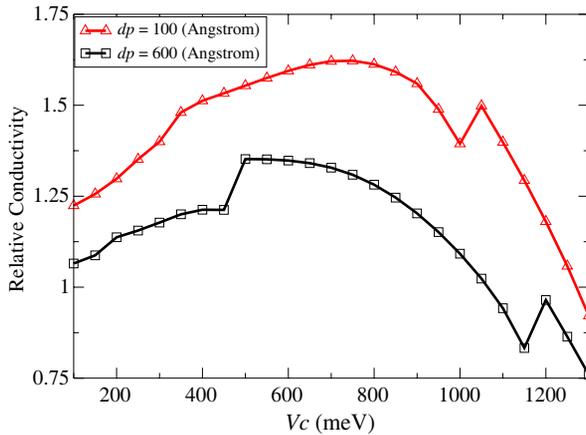
Figure 7. Relative conductivity as a function of potential of contact for two values of inter-well distance between the n-type well and the p-type barriers in ALD-FET in GaAs for $N_{2d} = 7.5 \times 10^{12} \, \mathrm{cm}^{-2}$, $p_{2d} = 5 \times 10^{13} \, \mathrm{cm}^{-2}$, $d_p = 100 \, \mathring{\mathrm{A}}$ (triangle up symbol), $d_p = 600 \, \mathring{\mathrm{A}}$ (square symbol).

In Figure 7, the evolution curves of the relative conductivity σ_{rel} are presented as a function of contact potential for two positions of the p-type delta doped barrier. The upper curve corresponds to $d_p = 100\,\text{Å}$, where a better conductivity is observed. For $d_p = 600\,\text{Å}$, we have a δ-FET behavior conductivity. The conductivity at each position operates almost in a similar way. It is noted that there are two types of regions: a) -The first type is constituted of two linear regions. In the case of $d_p = 100\,\text{Å}$, the first linear region is increasing in [100, 300], and the second linear region is decreasing in [1050, 1300] (all in meV). It is very important to define these linear regions in microelectronics, because they are the regions for which the transconductance is flat, or zones that ensure less distortion in the amplification [11, 14]. b) -The second type is a parabolic region, and it is located between 350 meV and 1050 meV for $d_p = 100\,\text{Å}$, and between 500 meV and 1150 meV for $d_p = 600\,\text{Å}$. In this region, the conductivity begins to decrease from the optimal point of conductivity, $V_c = 750$ meV for top curve, and from 500 meV for the lower curve. This means that the conduction channel begins to be narrow, due to the strong decrease of the confined electrons in delta doped well.

The ALD-FET permits to have a negative differential resistance (NDR) as other delta doped systems [40–43]. NDR can be seen in this device for the intervals in meV [500, 1150] and [1200, 1300] for $d_p = 600\,\text{Å}$ and for $d_p = 100\,\text{Å}$ in the intervals [750, 1000] and [1050, 1300].
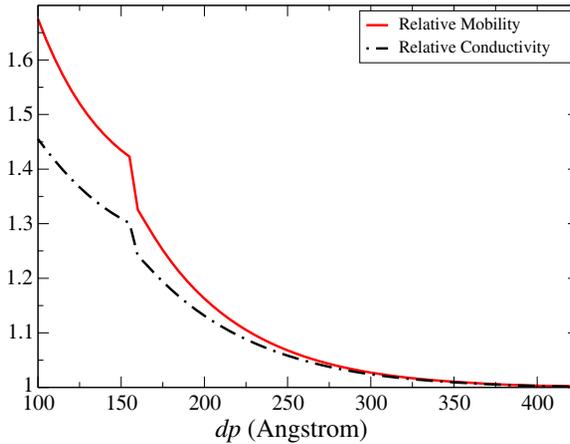
Figure 8. Relative mobility and conductivity versus the distance inter-well in ALD-FET in GaAs for $Vc = 500$ meV, $N_{2d} = 7.5 \times 10^{12}\,\text{cm}^{-2}$, $p_{2d} = 5 \times 10^{13}\,\text{cm}^{-2}$.

The regions where the ALD-FET operates with a negative differential resistance have a great importance in microelectronics. What is known in electronics is that an amplifier coupled with a properly designed positive feedback circuit can be made into an oscillator without input signal. For this reason, it is necessary to define the regions where the relative conductivity has a negative slope.

In the following, the transport for different positions of p-type δ-doped barrier will be analyzed. It is considered as a reference for the calculation of the relative mobility the position of the barrier to infinity, $d_p = +\infty$ (δ-FET case), also it is considered $V_c = 500$ meV.

In Figure 8, the behavior of mobility vs. d_p and conductivity vs. d_p is shown. It can be observed that the relative mobility decreases strongly from 1.67 to 1.31 between 100 Å and 160 Å. And it decreases slowly from 1.31 to 1 between 160 Å and 400 Å. On the other hand, the transition in the mobility and conductivity between 155 Å and 160 Å is the result of changing the number of energy levels of the electronic structure. For $d_p \geqslant 400$ Å it can be considered that we have a δ-FET and not a ALD-FET transistor. In other words, the p-type delta doped barrier does not have effect on the mobility and conductivity. From these results, it can be concluded that the transport phenomenon (mobility and conductivity) is better in ALD-FET than in δ-FET.
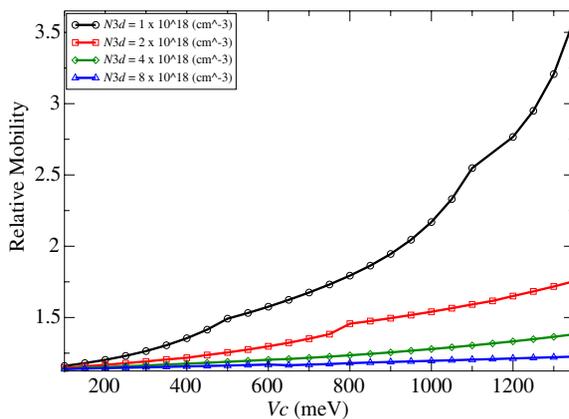
Figure 9. Relative mobility as a function of contact voltage for different values of background density, $N_d = 1 \times 10^{18}$ cm^{-3}, $N_d = 2 \times 10^{18}$ cm^{-3}, $N_d = 4 \times 10^{18}$ cm^{-3}, and $N_d = 8 \times 10^{18}$ cm^{-3} for $N_{2d} = 7.5 \times 10^{12}$ cm^{-2}, $p_{2d} = 5 \times 10^{13}$ cm^{-2} in ALD-FET in GaAs. Inter-well distance between the n-type well and the p-type barriers is $d_p = 300$ Å. Distance at which the n-type δ-doped well is positioned is $d = 300$ Å.

Let us see the Ohmic region dependent on the background density. Figure 9 presents the behavior of mobility for the ALD-FET in GaAs. It can be noted that the slopes of mobility decrease when the density of background impurities increase. In Figure 10, the relative conductivity evolution is presented as a function of the contact potential for different values of background density.

One of the most important aspects found in this calculation is that the Ohmic region properties depend on the density of background impurities.

When the density is equal to $N_d = 1 \times 10^{18}\,\mathrm{cm}^{-3}$ the Ohmic region is located in the interval [50, 600] (in meV). For $N_d = 2 \times 10^{18}\,\mathrm{cm}^{-3}$ the Ohmic region is duplicated and when the density is bigger than $N_d = 8 \times 10^{18}\,\mathrm{cm}^{-3}$ a long Ohmic region appears between 50 meV and 1400 meV. Moreover, the slopes of the Ohmic region decrease when the background density increases. It is precisely this behavior of Ohmic region that allows this device to achieve a stable electronic amplification. Results of the calculation in Figure 10 allow us to conclude that the density of impurities plays a special role in determining the nature of the Ohmic region.
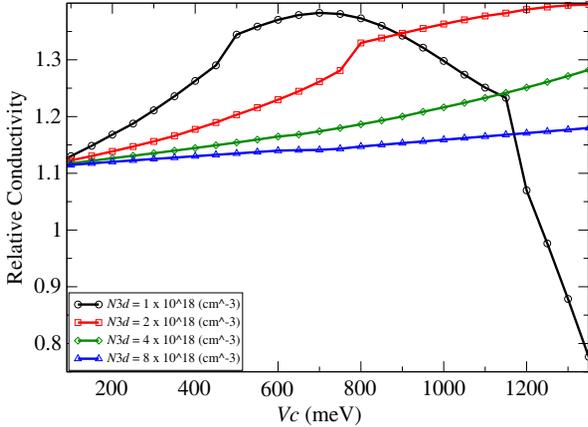
Figure 10. Relative conductivity as a function of contact voltage for different values of background density, $N_d = 1 \times 10^{18}\,\mathrm{cm}^{-3}$, $N_d = 2 \times 10^{18}\,\mathrm{cm}^{-3}$, $N_d = 4 \times 10^{18}\,\mathrm{cm}^{-3}$, and $N_d = 8 \times 10^{18}\,\mathrm{cm}^{-3}$ for $N_{2d} = 7.5 \times 10^{12}\,\mathrm{cm}^{-2}$, $p_{2d} = 5 \times 10^{13}\,\mathrm{cm}^{-2}$ in ALD-FET in GaAs. Inter-well distance between the n-type well and the p-type barriers is $d_p = 300\,\text{Å}$. Distance at which the n-type δ-doped well is positioned is $d = 300\,\text{Å}$.
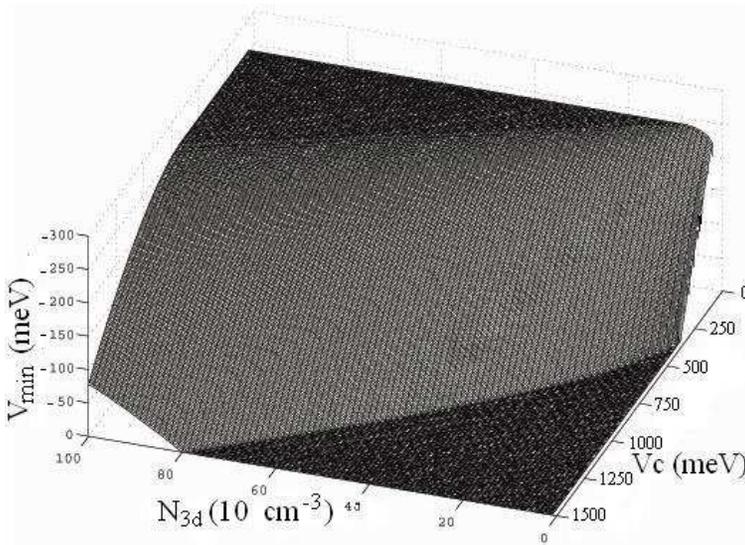
Figure 11. Bottom of the n-type δ-doped well $V_{\min}$ vs. N_d and V_c for $d_p = 300\,\text{Å}$ and $p_{2d} = 5 \times 10^{13}\,\text{cm}^{-2}$.

Figure 11 shows the bottom of the conduction channel as a function of contact potential and background impurity density. The bi-dimensional impurity concentration and the distance have fixed values. In this figure, two interesting dark areas can be observed. The upper dark area shows the conducting channel when the channel is open, which means that for a given background density, the conduction channel does not feel the effects of the contact potential. The dark area below represents a closed conducting channel, when the potential of the conduction channel bottom is zero. This result could be compared qualitatively to the analysis given in [44], where no quantum states are observed for back ground impurity concentration of $7 \times 10^{16}\,\text{cm}^{-3}$. In this type of transistors, the two dark areas allow to identify the digital operation mode of the system. In other words, when the conduction channel is open (dark area above) the transistor is saturated, and when the conduction channel is closed (dark area below) the transistor is blocked.

The intermediate region between the two dark areas predicts the alteration of the well bottom by the presence of the Schottky barrier. For a given background density N_d, this region will be determined by the following inequality $6.8 \times 10^{-16}N_d + 18.2\,\text{meV}$ $\leq V_c \leq -0.05(N_d \times 10^{-16} - 162.3)^2 + 1886\,\text{meV}$, where N_d in cm^{-3}
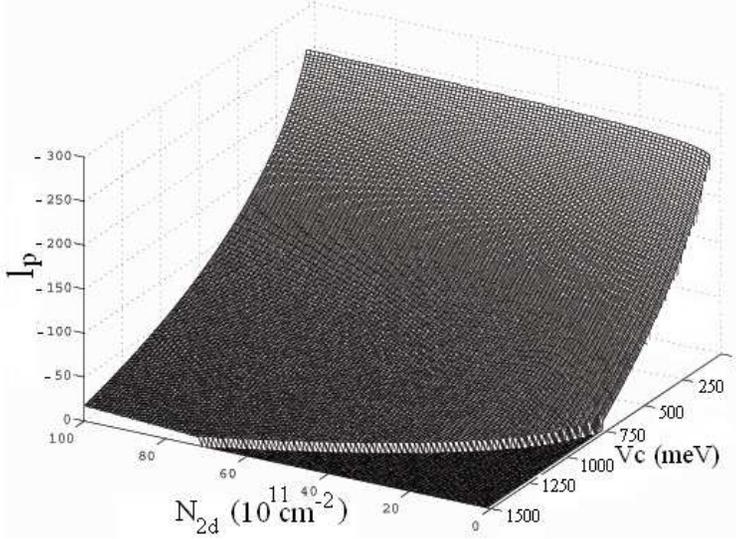
Figure 12. Depletion region l_p in Å vs. N_{2d} and V_c for $d_p = 300\,\text{Å}$ and $p_{2d} = 5 \times 10^{13}\,\text{cm}^{-2}$.

and V_c in meV. In this intermediate region it can be seen that the transistor could be operated in analogue mode.

Another way to identify the system mode operation is analyzing the depletion region. Figure 12 shows the behavior of depletion region versus the impurities density of the n-type δ-doped quantum-well N_{2d} in $10^{11}\,\text{cm}^{-2}$ and contact potential (V_c) in meV. From this figure, it is easy to infer the analogical mode where $V_c \leq -0.09(N_{2d} \times 10^{-11} - 90.7)^2 + 1490\,\text{meV}$.

5. CONCLUSIONS

We have found analytical expressions for transport phenomena that give satisfactory results for the mobility and the conductivity in ALD-FET devices. It is found that the Ohmic region is more outstanding with increasing the background density and that this device operates as NDR when contact potential is high. We had determined the ranges in which this system works in the digital or analogue mode. Finally, it is found that the ALD-FET device has better transport phenomenon than the δ-FET transistor in terms of mobility and conductivity. These results can be the basis for future work in other delta doped transistors.

ACKNOWLEDGMENT

REFERENCES

1. Zhu, C., J. K. O. Sin, and H. S. Hwok, "Characteristics of p- and n-channel poly-Si/Si$_{1-x}$Ge$_x$/Si sandwiched conductivity modulated thin-film transistors," *IEEE Trans. Electron Devices*, Vol. 47, No. 11, 2188–2193, 2000.

2. Schubert, E. F., A. Fischer, and K. Ploog, "The delta-doped field-effect transistor (δ-FET)," *IEEE Trans. Electron Devices*, Vol. 33, 625–632, 1986.

3. Chakhnakia, Z. D., L. V. Khvedelidze, N. P. Khuchua, R. G. Melkadze, G. Peradze, and T. B. Sakharova, "AlGaAs-GaAs heterostructure δ-doped field-effect transistor (δ-FET)," *Proc. SPIE.*, Vol. 5401, 354–361, 2004.

4. Lin, Y. M., S. L. Wu, S. J. Chang, S. Koh, and Y. Shiraki, "SiGe heterostructure field-effect transistor using V-shaped confining potential well," *IEEE Electron Device Lett.*, Vol. 24, No. 2, 69–71, 2003.

5. Aleksov, A., A. Denisenko, M. Kunze, A. Vescan, A. Bergmaier, G. Dollinger, W. Ebert, and E. Kohn, "Diamond diodes and transistors," *Semicond. Sci. Technol.*, Vol. 18, 59–66, 2003.

6. Abid, Z., A. Gopinath, B. Meskoob, and S. Prasad, "GaAs MESFETs with channel-doping variations," *Solid-State Electron.*, Vol. 34, No. 12, 1427–1432, 1991.

7. Ueda, K., M. Kasu, Y. Yamauchi, T. Makimoto, M. Schwitters, D. J. Twitchen, G. A. Scarsbrook, and S. E. Coe, "Diamond FET using high-quality polycrystalline diamond with f_T of 45 GHz and $f_{\max}$ of 120 GHz," *IEEE Electron Device Lett.*, Vol. 27, No. 7, 2006.

8. Wort, C. J. H. and R. S. Balmer, "Diamond as an electronic material," *Mater. Today*, Vol. 11, Nos. 1–2, 22–28, 2008.

9. Balmer, R. S., I. Friel, S. M. Woollard, C. J. H. Wort, G. A. Scarsbrook, S. E. Coe, H. El-Hajj, A. Kaiser, A. Denisenko, E. Kohn, and J. Isberg, "Unlocking diamonds potential as an electronic material," *Phil. Trans. R. Soc. A*, Vol. 366, 251–265, 2008.

10. El-Hajj, H., A. Denisenko, A. Kaiser, R. S. Balmer, and E. Kohn, "Diamond MISFET based on boron delta-doped channel," *Diamond Relat. Mater.*, Vol. 17, 1259–1263, 2008.

11. Nakajima, S., N. Kuwata, N. Shiga, K. Otobe, K. Matsuzaki, T. Sekiguchi, and H. Hayashi, "Characterization of double pulse-doped channel GaAs MESFETs," *IEEE Trans. Electron Devices*, Vol. 14, No. 3, 146–148, 1993.

12. Balmer, R. S., J. R. Brandon, S. L. Clewes, H. K. Dhillon, J. M. Dodson, I. Friel, P. N. Inglis, T. D. Madgwick, M. L. Markham, T. P. Mollart, N. Perkins, G. A. Scarsbrook, D. J. Twitchen, A. J. Whitehead, J. J. Wilman, and S. M. Woollard, "Chemical vapour deposition synthetic diamond: materials, technology and applications," *J. Phys.: Condens. Matter.*, Vol. 21, No. 36, 364221, 2009.

13. Yamaguchi, K., Y. Shiraki, Y. Katayama, and Y. Murayamn, "A new short channel MOSFET with an atomic-layer-doped impurity-profile (ALD-MOSFET)," *Jpn. J. Appl. Phys.*, Vol. 22, 267–270, Supplement 22-1, 1983.

14. Lien, C., Y. Huang, H. Chien, and W. Wang, "Charge control model of the double delta-doped quantum-well field-effect transistor," *IEEE Trans. Electron Devices*, Vol. 41, No. 8, 1351–1356, 1994.

15. Miyao, M., K. Nakagawa, H. Nakahara, Y. Kiyota, and M. Kondo, "Recent progress of heterostructure technologies for novel silicon devices," *Appl. Surf. Sci.*, Vol. 102, No. 2, 360–371, 1996.

16. Martínez-Orozco, J. C., I. Rodríguez-Vargas, C. A. Duque, M. E. Mora-Ramos, and L. M. Gaggero-Sager, "Study of the electronic properties of GaAs-based atomic layer doped field effect transistor (ALD-FET) under the influence of hydrostatic pressure," *Phys. Status Solidi B*, Vol. 246, No. 3, 581–585, 2009.

17. Aleksov, A., M. Kubovic, N. Kaeb, U. Spitzberg, A. Bergmaier, G. Dollinger, T. Bauer, M. Schreck, B. Stritzker, and E. Kohn, "Diamond field effect transistors concepts and challenges," *Diamond Relat. Mater.*, Vol. 12, Nos. 3–7, 391–398, 2003.

18. Zeindl, H. P., B. Bullemer, I. Eisele, and G. Tempel, "Delta-doped MESFET with MBE-grown Si," *J. Electrochem. Soc.*, Vol. 136, No. 4, 1129–1131, 1989.

19. Nakagawa, K., A. A. van Gorkum, and Y. Shiraki, "Atomic layer doped field effect transistor fabricated using Si molecular beam epitaxy," *Appl. Phys. Lett.*, Vol. 54, No. 19, 1869–1871, 1989.

20. Oubram, O., L. M. Gaggero-Sager, and D. S. Díaz-Guerrero, "Relative mobility and relative conductivity in ALD-FET (Atomic layer doped-field effect transistor) in GaAs," *PIERS Proceeding.*, 1186–1190, Beijing, China, Mar. 23–27, 2009.

21. Mora-Ramos, M. E. and L. M. Gaggero-Sager, "A simple

model for atomic layer doped field-effect transistor (ALD-FET) electronic states," *Rev. Mex. Fís.*, Vol. 44, No. 3, 165–167, 1998.

22. Oubram, O. and L. M. Gaggero-Sager, "Transport properties of delta-doped field effect transistor," *Progress In Electromagnetics Research Letters*, Vol. 2, 81–87, 2008.

23. Gaggero-Sager, L. M. and R. Perez-Alvarez, "A simple model for delta doped field effect transistor electronic states," *J. Appl. Phys.*, Vol. 78, No. 7, 4566–4569, 1995.

24. Oubram, O., L. M. Gaggero-Sager, A. Bassam, and G. A. Luna Acosta, "Transport and electronic properties of two dimensional electron gas in delta-migfet in GaAs," *Progress In Electromagnetics Research*, Vol. 110, 59–80, 2010.

25. Ozturk, E., "Effect of magnetic field on a p-Type δ-doped GaAs layer," *Chinese Phys. Lett.*, Vol. 27, 2010.

26. Ozturk, E., "Optical intersubband transitions in double Si δ-doped GaAs under an applied magnetic field," *Superlattices Microstruct.*, Vol. 46, No. 5, 752–759, 2009.

27. Ozturk, E., M. K. Bahar, and I. Sokmen, "Subband structure of p-type δ-doped GaAs as dependent on the acceptor concentration and the layer thickness," *Eur. Phys. J. Appl. Phys.*, Vol. 41, 195–200, 2008.

28. El-Hajj, H., A. Denisenko, A. Bergmaier, G. Dollinger, M. Kubovic, and E. Kohn, "Characteristics of boron δ-doped diamond for electronic applications," *Diamond Relat. Mater.*, Vol. 17, 409–414, 2008.

29. Chen, X. and B. Nabet, "A closed-form expression to analyze electronic properties in delta-doped heterostructures," *Solid-State Electron.*, Vol. 48, 2321–2327, 2004.

30. Rhoderick, E. H. and R. H. Williams, *Metal-semiconductor Contacts*, Clarendon Press, Oxford, 1988.

31. Ioriatti, L., "Thomas-Fermi theory of δ-doped semiconductor structures: Exact analytical results in the high-density limit," *Phys. Rev. B.*, Vol. 41, 8340–8344, 1990.

32. Gaggero-Sager, L. M., R. Mora-Ramos, and D. A. Contreras-Solorio, "Thomas-Fermi approximation in p-type δ-doped quantum wells of GaAs and Si," *Phys. Rev. B.*, Vol. 57, No. 11, 6286–6289, 1998.

33. Rodríguez-Vargas, I., L. M. Gaggero-Sager, and V. R. Velasco, "Thomas-Fermi-Dirac theory of the hole gas of a double p-type δ-doped GaAs quantum wells," *Surf. Sci.*, Vol. 537, Nos. 1–3, 75–83, 2003.

34. Wu, C. J. and Z. H. Wang, "Properties of defect modes in one-dimensional photonic crystals," *Progress In Electromagnetics Research*, Vol. 103, 169–184, 2010.

35. Banerjee, A., "Enhanced refractometric optical sensing by using one-dimensional ternary photonic crystals," *Progress In Electromagnetics Research*, Vol. 89, 11-22, 2009.

36. Rahimi, H., A. Namdar, S. Roshan Entezar, and H. Tajalli, "Photonic transmission spectra in one-dimensional fibonacci multilayer structures containing single-negative metamaterials," *Progress In Electromagnetics Research*, Vol. 102, 15–30, 2010.

37. Wu, C.-J., Y.-H. Chung, B.-J. Syu, and T.-J. Yang, "Band gap extension in a one-dimensional ternary metal-dielectric photonic crystal," *Progress In Electromagnetics Research*, Vol. 102, 81–93, 2010.

38. Wu, C.-J., Y.-N. Rau, and W.-H. Han, "Enhancement of photonic band gap in a disordered quarter-wave dielectric photonic crystal," *Progress In Electromagnetics Research*, Vol. 100, 27–36, 2010.

39. Tuz, V. R. and C.-W. Qiu, "Semi-infinite chiral nihility photonics: Parametric dependence, wave tunneling and rejection," *Progress In Electromagnetics Research*, Vol. 103, 139–152, 2010.

40. Wang, Y. H., "Interband resonant tunneling diode in δ-doped GaAs," *Appl. Phys. Lett.*, Vol. 57, No. 15, 1546–1547, 1990.

41. Sardela, Jr., M. R., H. H. Radamson, L. Hultman, and G. V. Hansson, "Growth, characterization and device fabrication of Boron delta-doped structures by Si-molecular beam epitaxy," *Jpn. J. Appl.*, Vol. 33, 2279–2281, 1994.

42. Li, S. M., W. M. Zheng, A. L. Wu, W. Y. Cong, J. Liu, N. N. Chu, and Y. X. Song, "Terahertz electroluminescence from Be δ-doped GaAs/AlAs quantum well," *Appl. Phys. Lett.*, Vol. 97, No. 2, 023507-1–023507-2, 2010.

43. Weng, T. Y., J. H. Tsai, and D. F. Guo, "An optoelectronic switch with multiple operation states," *IEEE, Optoelectronic and Microelectronic Materials and Devices, Conference*, 90–93, 2006.

44. Geraldo, J. M., W. N. Rodrigues, G. Medeiros-Ribeiro, and A. G. de Oliveira, "The effect of the planar doping on the electrical transport properties at the Al:n-GaAs (100) interface: Ultrahigh effective doping," *J. Appl. Phys.*, Vol. 73, No. 2, 820–823, 1993.